Computers and Concrete, *Vol. 13, No. 5 (2014) 633-648*
DOI: http://dx.doi.org/10.12989/cac.2014.13.5.633

Earthquake safety assessment of an arch dam using an anisotropic damage model for mass concrete

Xinhua Xue* and Xingguo Yang

State Key Laboratory of Hydraulics and Mountain River Engineering, College of Water Resource and Hydropower, Sichuan University, No.24 South Section 1, Yihuan Road, Chengdu, Sichuan, 610065, P.R.China

(*Received November 13, 2013, Revised April 11, 2014, Accepted May 22, 2014*

Abstract. The seismic safety of concrete dams is one of the important problems in the engineering due to the vast socio-economic disasters which may be caused by collapse of these infrastructures. The accuracy of the risk evaluation associated with these existing dams as well as the efficient design of future dams is highly dependent on a proper understanding of their behaviour due to earthquakes. This paper develops an anisotropic damage model for arch dam under strong earthquakes. The modified Drucker-Prager criterion is adopted as the failure criteria of the dynamic damage evolution of concrete. Some process fields and other necessary information for the safety evaluation are obtained. The numerical results show that the seismic behaviour of concrete dams can be satisfactorily predicted.

Keywords: damage analysis; high-arch dam; seismic response; safety evaluation

1. Introduction

The seismic safety of arch dam is a widely discussed topic because the failure of an arch dam can result in unimaginable loss of human lives and substantial property damage (Wang *et al*. 2011). The accuracy of the risk evaluation associated with these existing dams as well as the efficient design of future dams is highly dependent on a proper understanding of their behaviour due to earthquakes (Valliappan *et al*. 1999). Because of the large differences between the design acceleration and the peak ground accelerations (PGA), which can actually occur during a strong earthquake, and because of the uncertainties in estimating the ground motion of very strong earthquakes at a dam site, mechanisms are needed that ensure that a dam will not fail if the design acceleration is exceeded substantially. Although many studies have been done on the earthquake behaviour of arch dams by many researchers, past and present (Sevim *et al*. 2011; Akköse *et al*. 2007; Oliveira and Faria 2006; Alves and Hall 2006; Shahkarami *et al*. 2004; Lotfi and Espander 2004; Du *et al*. 2009), however, because of the lack of experimental and practical results and also because of existing differences between the results obtained from different numerical models, it is difficult to choose an appropriate numerical model to evaluate the seismic safety of dams (Mirzabozorg and Ghaemian 2005). Therefore, it is still necessary to develop analytical procedures

*Corresponding author, Associate professor, E-mail: scuxxh@163.com

 ISSN: 1598-8198 (Print), 1598-818X (Online)

for evaluating the adequacy of a given design against a particular ground motion.

It is well known that the damage of concrete and foundation rock body as quasi-brittle non-homogeneous materials is a result of continuous developing of random distributed microcracks.

Although the simplicity and efficiency of a scalar damage representation is indeed very attractive, the orientation-independent isotropic damage variable is subsequently found to be inaccurate. It has been shown that the nucleation and growth of voids as well as the orientation of fissures and their lengths observed in the process of material damage depend significantly on the direction of the applied stresses or strains and, hence, damage is in general anisotropic. Some researchers have studied the seismic response of concrete dams using Continuum Damage Mechanics (CDM). Their results indicate that non-linear analysis based on CDM generally gives responses which fall within the realistic range but are also conservative. Chow and Wang (Chow and Wang 1988) reported that isotropic damage models usually predict lower strength of materials compared to the theory of anisotropic damage, and the importance of the directional nature of material damage in controlling final rupture becomes more pronounced under dynamic loading conditions. An analysis without taking into account the damage-induced material anisotropy may therefore lead to questionable results. Therefore, the main purpose of this article is to provide such a model in the framework of Continuum Damage Mechanics (CDM). The modified Drucker-Prager criterion is adopted as the failure criteria of the dynamic damage evolution of concrete. The numerical results show that the seismic behaviour of concrete dams can be satisfactorily predicted. This will provide a reasonable theoretical support on the safety evaluation of the capability for concrete arch dams against earthquake loading.

2. Damage stress-strain relationship

The constitutive relationship in the principal anisotropic coordinate system is presented as (Xue 2008)

$$\left\{\sigma^*\right\}=\left[D^*\right]\left\{\varepsilon^*\right\} \tag{1}$$

where $\left\{\sigma^*\right\}$ and $\left\{\varepsilon^*\right\}$ are Cauchy stress and Cauchy strain. $\left[D^*\right]$ is stiffness with the influence of anistropic damage.

$$\left[D^*\right]=\begin{bmatrix} d_{11}^* & d_{12}^* & d_{13}^* & 0 & 0 & 0 \\ d_{21}^* & d_{22}^* & d_{23}^* & 0 & 0 & 0 \\ d_{31}^* & d_{32}^* & d_{33}^* & 0 & 0 & 0 \\ 0 & 0 & 0 & g_{12}^* & 0 & 0 \\ 0 & 0 & 0 & 0 & g_{23}^* & 0 \\ 0 & 0 & 0 & 0 & 0 & g_{31}^* \end{bmatrix} \tag{2}$$

in which

$$
\begin{aligned}
d_{ii}^{*} &= \frac{d_i^{*}\left(1-v_{jk}^{*}v_{kj}^{*}\right)}{\Delta} \quad \left(j \neq i\right) \\
d_{ij}^{*} &= \frac{d_i^{*}\left(v_{ji}^{*}+v_{ki}^{*}v_{jk}^{*}\right)}{\Delta} \quad \left(i \neq j, k \neq i, j \neq k\right) \\
\Delta &= 1-v_{12}^{*}v_{21}^{*}-v_{23}^{*}v_{32}^{*}-v_{13}^{*}v_{31}^{*}-2v_{21}^{*}v_{32}^{*}v_{13}^{*}
\end{aligned} \tag{3}
$$

also

$$
\begin{aligned}
d_i^{*} &= \left(1-\Omega_i\right)^2 d_i \\
v_{ij}^{*} &= \frac{1-\Omega_i}{1-\Omega_j} v_{ij} \\
g_{ij}^{*} &= \frac{2\left(1-\Omega_i\right)^2\left(1-\Omega_j\right)^2}{\left(1-\Omega_i\right)^2+\left(1-\Omega_j\right)^2} g_{ij}
\end{aligned} \tag{4}
$$

in which Ω_i, i =1, 2, 3 are the principal values of damage tensor. In the case of brittle materials, the constitutive relationships defined above have to be modified depending on whether the principle stresses are tensile or compressive, for example, in the case of compressive principal, undamaged properties will be adopted.

3. Damage evolution equation

It is well known that concrete and geomaterials eventually exhibit strain softening, leading to a complete loss of strength. In these materials, the secant modulus decreases with increasing strain (Lubliner *et al*. 1989). A widely used assumption has been to adopt a triangular stress-strain diagram for uniaxial loading. This gives a linear strain softening relationship. But various experimental evidences indicate that it is more realistic to assume a strain softening curve with a steep initial decline followed by an extended tail (Lubliner *et al*. 1989). Thus, an exponential strain softening model yields

$$
\sigma\left(\varepsilon\right) = \begin{cases} D\varepsilon & \varepsilon \leq \varepsilon_0 \\ f_t'\left[2\exp\left(-a\left(\varepsilon-\varepsilon_0\right)\right)-\exp\left(-2a\left(\varepsilon-\varepsilon_0\right)\right)\right] & \varepsilon_0 < \varepsilon < \varepsilon_{cr} \\ 0 & \varepsilon \geq \varepsilon_{cr} \end{cases} \tag{5}
$$

where f_t' is the tensile strength and ε_0 is the corresponding strain threshold, D is the modulus of elasticity and a is a dimensionless constant. In the above relations, a maximum strain ε_{cr} has been adopted that may not be exceeded in strain softening, and is consistent with the study carried out by Bazant (1987). In the present study, the value of ε_{cr} is calculated when its corresponding stress

is equal to 0.02 f_t', which is a reasonable value.

Based on the hypothesis of strain energy equivalence, the anisotropic damage parameters can be defined in terms of Young's modulus as

$$\Omega_i = 1 - \sqrt{\frac{D_i^*}{D_i}} \tag{6}$$

Hence, from equation (5) the proper definition of damage variable for uniaxial case is (Valliappan *et al*. 1999)

$$\Omega = 1 - \sqrt{\left(\frac{\varepsilon_0}{\varepsilon}\right)\left[2\exp\left(-a\left(\varepsilon-\varepsilon_0\right)\right) - \exp\left(-2a\left(\varepsilon-\varepsilon_0\right)\right)\right]} \tag{7}$$

It should be noted that in the case of three dimensions, there will be three damage variables in the three principal directions.

Earthquake loading being cyclic, when the sign of the stresses change from tension to compression, cracks tend to close. During this change, concrete cannot recover all of its deformation. Dahlblom and Ottosen (1990) introduced a fraction δ =0.2 of the maximum developed principal strain to be inelastic. Hence the total strain is divided into two parts: elastic ε_e and inelastic ε_{in}:

$$\varepsilon = \varepsilon_e + \varepsilon_{in} = \varepsilon_e + \delta\varepsilon_{\max} \tag{8}$$

It should be pointed out that equation (8) applies to the principal strains and in 3-D, there will be three such equations. Also, when the stress state changes from tension to compression, the maximum tensile principal strain obtained before will remain the same and due to closure of cracks, the material is assumed to have its original stiffness characteristics. Reloading of the crack follows the unloading path until the principal strain is greater than $\varepsilon_{\max}$. Also when the strain is less than ε_{in} it is supposed that the crack is closed.

The constitutive law and the damage model described in the previous sections have been implemented in a dynamic Lagrangian non-linear finite element code. In this method, the damage evolution in each element can be determined, thus making it possible to model both damage propagation and damage growth. The stress-strain law adopted for the brittle materials is as follows: the local definition of damage variable for each point is slightly modified to refer to the behaviour of an element. The strains are computed at each integration point and the average at the Gaussian point is taken as the representative behaviour of the whole element. It is assumed that cracking initiates at a point when the maximum tensile principal strain is greater than ε_0. The direction of a crack is assumed to be orthogonal to that of the maximum tensile principal stress at the damaged point. After computing the total displacement at every iteration, the strains are calculated and averaged at the center of an element and then its corresponding principal strains are determined. Next, two different cases may happen (Valliappan *et al*.1999):

(1) If the element is already damaged during last time steps, depending on the value of the principal strain, ε, three different cases may arise:

① If $\varepsilon \geq \varepsilon_{\max}$, the element is in a loading stage. Calculate damage value from equation (7), update $\varepsilon_{in} = \delta\varepsilon$ and $\varepsilon_{\max} = \varepsilon$.

② If $\varepsilon_{in} \leq \varepsilon \leq \varepsilon_{\max}$, the element is in an unloading stage, but cracks are open. Use damage value at previous time step as a current damage: $\Omega = \Omega_{old}$.

③ If $\varepsilon \leq \varepsilon_{in}$, the cracks are closed and the element is in compression. Assume undamaged state in calculations.

(2) If the element is not damaged and the principal strain is less than ε_0, elastic properties for the undamaged element should be used. Otherwise, if $\varepsilon > \varepsilon_0$, among all the candidate elements that would initiates softening at a particular iteration, the one with highest tensile strain energy density is used first. Then, just one new softening element per iteration is allowed, i.e. several iterations may be performed in a particular time step. After calculating the damage variable, the constitutive matrix and the stresses are calculated.

4. Modification of drucker-prager criterion

According to the classical plasticity theory, the yield criterion determines the stress level at which plastic deformation begins. The damage plastic yield criterion can also be defined in a similar manner such that the yield condition determines the effective (net) stress level at which plastic deformation begins. This means that it is only necessary to replace the Cauchy stresses in the standard yield function by the effective stresses. The damage plastic yield function can be rewritten in the general form as

$$F\left(\{\sigma\}, \Omega, R\right) = F\left\{\left\{\sigma^*\right\}, R\right\} = 0 \tag{9a}$$

or

$$f\left(\{\sigma\}, \Omega\right) = f\left\{\left\{\sigma^*\right\}\right\} = R(\gamma) \tag{9b}$$

where f is a function to be used to determine the effective stress level at which the plastic deformation begins. $R(\gamma)$ is the hardening function associated with the cumulative hardening parameter γ. Commonly, the hardening rule can be considered as the power rule

$$R(\gamma) = R_0 + k\gamma^{\frac{1}{m}} \tag{10}$$

The damage yield function can conveniently be expressed in the form of stress invariants as

$$f\left(I_1^*, J_2^*, J_3^*\right) = R(\gamma) \tag{11}$$

where

$$I_1^* = \sigma_x^* + \sigma_y^* + \sigma_z^* = \frac{3\sigma_m}{1-\Omega} \tag{12}$$

$$J_2^* = \frac{1}{2}\left(s_x^* + s_y^* + s_z^*\right) + \sigma_{yz}^*\sigma_{zy}^* + \sigma_{zx}^*\sigma_{xz}^* + \sigma_{xy}^*\sigma_{yx}^* = \frac{J_2}{\left(1-\Omega\right)^2} \tag{13}$$

$$J_3^* = Det\begin{bmatrix} s_x^* & \sigma_{xy}^* & \sigma_{xz}^* \\ \sigma_{yx}^* & s_y^* & \sigma_{yz}^* \\ \sigma_{zx}^* & \sigma_{zy}^* & s_z^* \end{bmatrix} = \frac{J_3}{\left(1-\Omega\right)^3} \tag{14}$$

where I_1, J_2,J_3 are the first, second, third stress invariables, respectively. σ_m is the average stress.

For numerical computations, it is convenient to rewrite the yield function in terms of alternative stress invariants. The present formulation is modified based on Nayak and Zienkiewicz (Nayak and Zienkiewicz 1972) since its main advantage is that it permits the computer coding of the yield function and the flow rule in a general form and necessitates only the specification of three constants for any individual criterion. The effective principal stress vector can be given by summation of the effective deviatoric principal stress vector and the effective mean hydrostatic stress vector as

$$\begin{Bmatrix} \sigma_1^* \\ \sigma_2^* \\ \sigma_3^* \end{Bmatrix} = \frac{2\left(J_2^*\right)^{\frac{1}{2}}}{\sqrt{3}} \begin{Bmatrix} \sin\left(\theta^* - \frac{2\pi}{3}\right) \\ \sin\theta^* \\ \sin\left(\theta^* + \frac{4\pi}{3}\right) \end{Bmatrix} + \frac{I_1^*}{3}\begin{Bmatrix} 1 \\ 1 \\ 1 \end{Bmatrix} \tag{15}$$

where $\sigma_1^* > \sigma_2^* > \sigma_3^*$ and $-\pi/6 \le \theta^* \le \pi/6$. The term θ^* is essentially similar to the Lode angle.

The influence of a hydrostatic stress component on yielding was introduced by inclusion of an additional term in von Mises expression to give

$$F = \beta_o I_1^* + \left(J_2^*\right)^{\frac{1}{2}} - R\left(\gamma\right) = 0 \tag{16}$$

This yield surface has the form of a circular cone. In order to make the Drucker-Prager criterion with the inner or outer apices of the Mohr-Coulomb hexagon at any section, it can be shown that

$$\beta_o = \frac{2\sin\varphi}{\sqrt{3}\left(3 \pm \sin\varphi\right)} \tag{17}$$

$$R(\gamma)=\frac{6c\cos\varphi}{\sqrt{3}(3\pm\cos\varphi)} \tag{18}$$

where "+" for inner apice, "–" for outer apice. Substituting Eqs. (17), (18) into Eq. (16), it gives

$$F=\frac{2\sin\varphi}{\sqrt{3}(3\pm\sin\varphi)}I_1^*+\left(J_2^*\right)^{\frac{1}{2}}-\frac{6c\cos\varphi}{\sqrt{3}(3\pm\cos\varphi)}=0 \tag{19}$$

Substituting Eqs. (13) and (14) into Eq. (19), the modified Drucker-Prager criterion in terms of invariants of Cauchy stress deviator is represented as

$$F=\frac{2\sin\varphi}{\sqrt{3}(3\pm\sin\varphi)}I_1+\left(J_2\right)^{\frac{1}{2}}-\frac{6c\cos\varphi}{\sqrt{3}(3\pm\cos\varphi)}(1-\Omega)=0 \tag{20}$$

where the cohesion c also can be equivalently expressed by the hardening rule $R(\gamma)$ as

$$c=\frac{\sqrt{3}(3\pm\sin\varphi)}{6\cos\varphi}R(\gamma) \tag{21}$$

and when $\gamma=0$, it gives $R|_{\gamma=0}=R_0$, and $c|_{\gamma=0}=c_0=\sqrt{3}(3\pm\sin\varphi)/(6\cos\varphi)R_0$, we can obtain

$$c=c_0+\frac{\sqrt{3}(3\pm\sin\varphi)}{6\cos\varphi}k\gamma^{\frac{1}{m}} \tag{22}$$

5. Dynamic equilibrium equations

The equations of motion for the discretized dam for specified free-field ground acceleration are

$$\mathbf{M}\ddot{\mathbf{u}}+\mathbf{P}(\mathbf{u},\dot{\mathbf{u}})=-\mathbf{M}\mathbf{R}\ddot{\mathbf{u}}_{\mathbf{g}}+\mathbf{F}^{\mathrm{st}} \tag{23}$$

where u, $\dot{u}$, and $\ddot{u}$ are the displacement, velocity, and acceleration relative to the free-field ground motion, $\ddot{u}_g$; M is the mass matrix including the added mass for the reservoir, P is the restoring forces obtained from the finite element discretization, R is the influence matrix for $\ddot{u}_g$, and F^{st} are the static loads from self-weight of the dam and the hydrostatic pressure on the upstream face.

In the finite element analysis procedure, the restoring force P is assembled from the element contributions. For each element the restoring force, P_e is given by the integral of the stress field in the element domain V, as governed by the rate-dependent constitutive model:

$$\mathbf{P}_e(\mathbf{u},\dot{\mathbf{u}}) = \int_{V_e} \mathrm{N}^{\mathrm{T}}\boldsymbol{\sigma}\,\mathrm{d}\,\mathrm{V} + \int_{V_e} \mathrm{N}^{\mathrm{T}}\chi\,\mathrm{d}\,\mathrm{V} \tag{24}$$

where N is the matrix form of the strain-displacement operator, and χ is the contribution of the damping to the restoring stress.

The dam reservoir interaction problems can be analyzed using the three basic approaches: the Westergaard (1933), Euler and Lagrangian approaches. In the Westergaard approach, fluid-structure interaction is simply represented by an added mass attached to structure. In the Eulerian approach, displacements are variables in structure, while pressures are variables in fluid. Since the variables in fluid and structure are different, a special-purpose computer program for the solution of coupled systems is required. In the Lagrangian approach, variables in fluid and structure are identical. Hence, compatibility and equilibrium are automatically satisfied at nodes along interfaces between the fluid and the structure. This makes Lagrangian displacement-based fluid element very desirable since special interface equations are not required. However, the disadvantage of Lagrange is that the coordinate system can become severely distorted or tangled in an extremely deformed region, which can lead to adverse effects on the integration time step and accuracy. Because the added-mass concept for an incompressible reservoir has been used as the standard method in the earthquake response calculation of most dams and it gives a fair approximation of hydrodynamic pressure for many practical problems. Therefore, the hydrodynamic pressure due to dam-reservoir interaction is estimated using the Westergaard added mass technique in this study. The results obtained by Westergaard are very well approximated by (Bull 1994):

$$p^{'}(x) = \left[\frac{7}{8}\rho_w\sqrt{H(H-x)}\right]\ddot{u}_g \tag{25}$$

where ρ_w is the mass density, H the depth of reservoir and $\ddot{u}$ the imposed ground acceleration.

Having in mind the expressions for the inertia forces, the term inside the square bracket is usually called an added mass, and will be referred to as m_A.However, arch dams have surfaces with double curvature and the acceleration, $\ddot{u}_g$, is generally not normal to the surface, so it is necessary to perform some modifications in Eq. (25) before it can be applied.

Considering a point at the dam-reservoir interface, where $\underline{\mathrm{n}}$ denotes the normal unit vector to the dam surface and $\underline{\ddot{u}}_g$ the total acceleration, the corresponding normal acceleration, $\underline{\ddot{u}}_g$, can be obtained by:

$$\underline{\ddot{\mathrm{u}}}_{\mathrm{g}}^{\mathrm{n}} = \underline{\ddot{\mathrm{u}}}_{\mathrm{g}}\cos(\underline{\mathrm{e}},\underline{\mathrm{n}})\underline{\mathrm{n}} \tag{26}$$

where $\underline{\ddot{u}}_g / \left\|\underline{\ddot{u}}_g\right\|$

So, the hydrodynamic pressure, $\underline{p}$, can be evaluated as:

$$\underline{p} = \mathrm{m}_A\,\underline{\ddot{u}}_g^{\mathrm{n}} \tag{27}$$

With this pressure at the upstream face of a given finite element, the corresponding vector of

nodal forces permits the calculation of the additional mass of water at each nodal point. This mass is then added to the mass matrix previously determined for the concrete, to constitute the mass matrix of the ensemble dam and reservoir.

Based on the above mentioned formulations, the finite element computer code DADAP (Dam Anisotropic Damage Analysis Program) was written and compiled and adopted to verify the accuracy of the modeling.

6. Case study

The Buxi arch dam which is 145m in height and 237m in arc length of the dam crest is analyzed. The thicknesses at the crest and base (maximum) of the dam are 6 and 30 m, respectively. The normal depth of reservoir water is 143 m. The dam is located in a seismic region with horizontal peak ground acceleration on rock of 0.243g (Dang 2008). Safety evaluation of the dam subjected to the design earthquake is a crucial factor for the project. As we know that, the dam safety is controlled by the tensile stresses during earthquakes, while compressive stresses usually do not approach the compressive strength of concrete in most cases. Consequently, for simplification, only the tensile damage of concrete is considered in this study.

The time history curve of earthquake acceleration is shown in Fig. 1. The model of the Buxi arch dam can be found in Fig. 2. As shown in Fig. 2, 8-node solid elements with 2×2×2 Gauss integration are applied in the finite element discretization of the dam-foundation system. The 8-node solid elements have three degrees of freedom at each node that are translated in the *x*,*y*, and *z* directions. The total number of elements in the dam-foundation system is 6772. In this model, if the height of the dam is indicated as "H", the foundation is extended as "4H" in the transverse river direction, "2.5H" in the downstream direction and "2H" in the gravity direction. The foundation rock is assumed as linear elastic. The density of the dam ρ=2700kg/m^3, Poisson's ratio v=0.17, cohesion c=2.72MPa, friction angle of concrete φ=53.9°. The density of rock foundation ρ=2700kg/m^3, and Poisson's ratio v=0.25. The elastic moduli of rock foundation and concrete are 20 and 25GPa, respectively. The tensile strength f_t' is 1.5MPa (Dang 2008). For a dynamic analysis, the damping χ in the numerical simulation should attempt to reproduce the energy losses in the system when subjected to dynamic loading. In rock and concrete, material damping is mainly hysteretic (i.e. independent of frequency), but it is difficult to reproduce this type of damping numerically because of the problem with path dependence. Traditionally, the typical values of intrinsic damping used by the structural engineers are 2% for steel and 5% for concrete building (Nor and Abdul, 2010). Therefore, a 5% structural damping ratio is assumed in the analyses.

It is necessary to study on the natural vibration properties of the arch dam before dynamic analysis. After calculation, the first four order natural frequencies under the normal storage level can be obtained and they are listed as follows: 1.6196Hz, 1.9611Hz, 2.5765Hz, and 3.0716Hz, respectively. Fig. 3 shows the corresponding mode shapes. From here we can see that the first order mode (along the stream direction) plays a principal role in the whole dynamic analysis. Consequently, for simplification, only the results along the stream direction are considered in this study.

Fig. 4 shows the contours of displacements in stream direction distributed on the face of upstream at time 9.2s. The calculated results in Fig. 4 show that the maximum displacement in

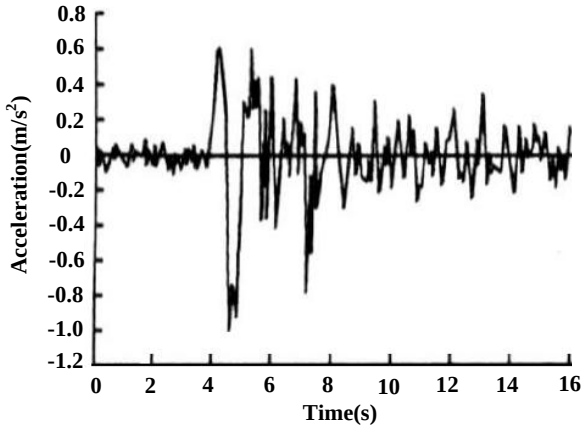

(a)

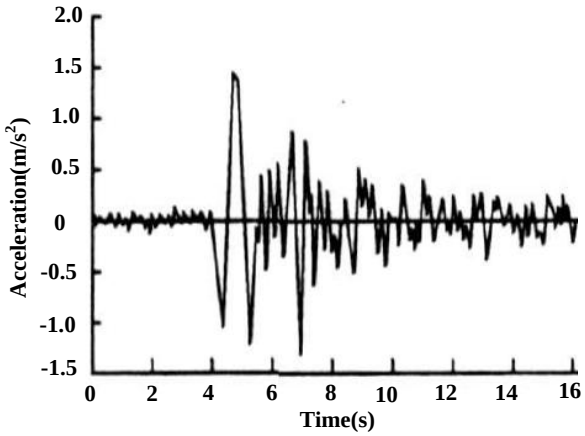

(b)

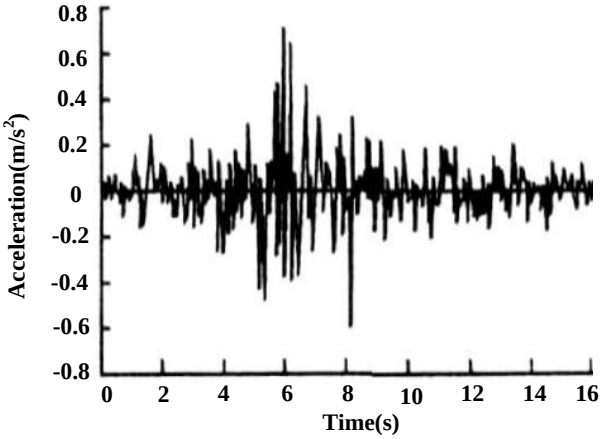

(c)

Fig.1 The acceleration components of the design earthquake across the river (a) , along the river (b) and in vertical direction (c) (unit: m/s^2)

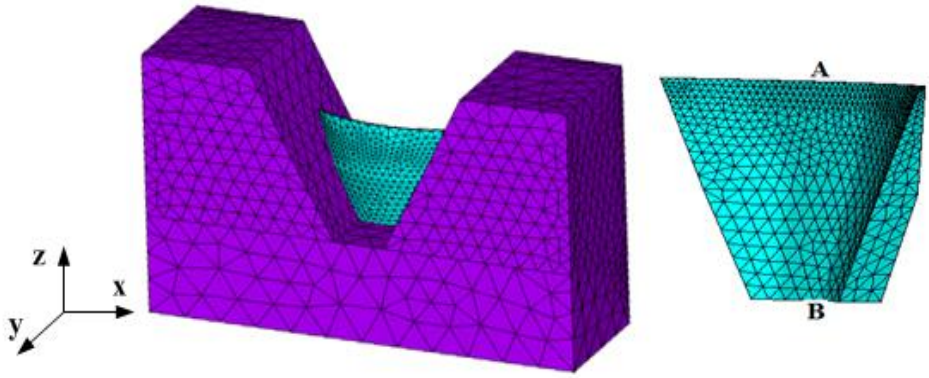

Fig. 2 The model of Buxi arch dam

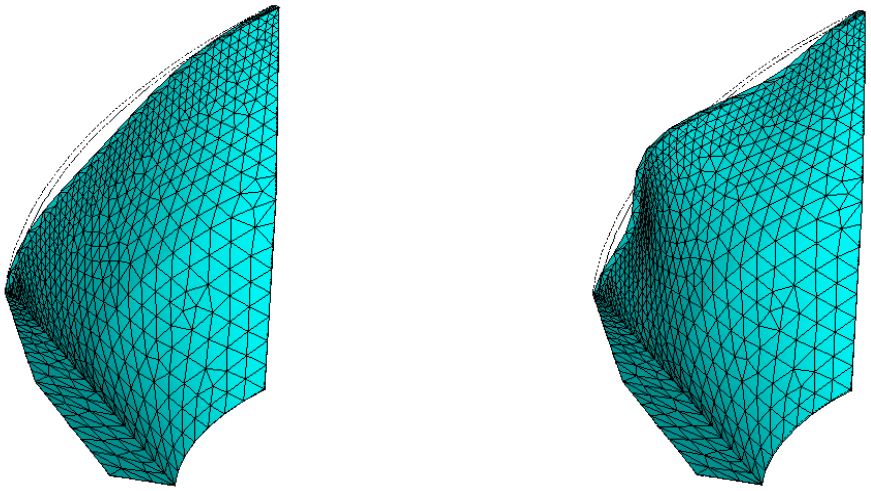

(a) First order mode (b) Second order mode

(c) Third order mode (d) Fourth order mode

Fig. 3 The first four lower-order modes of Buxi arch dam

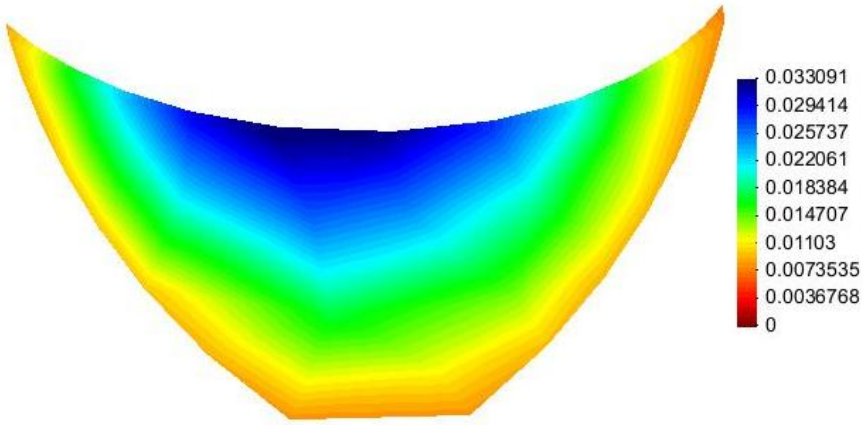

Fig. 4 Contours of u distributed on the face of upstream at time 9.2s (Unit: m)

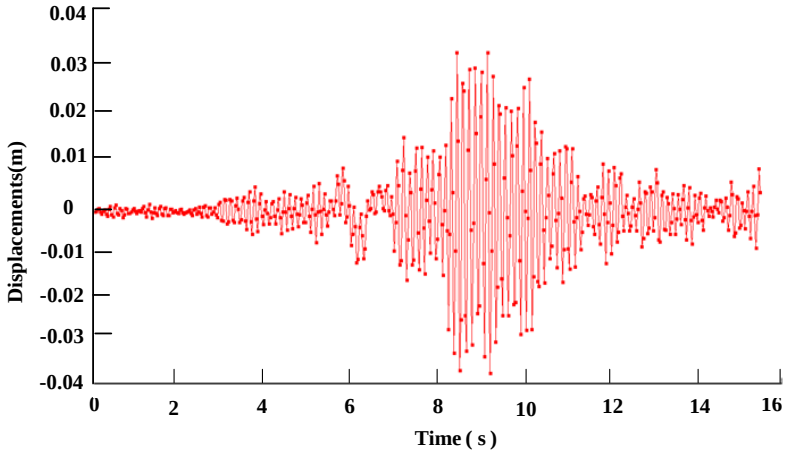

Fig. 5 Time-displacement curve of point A in stream direction

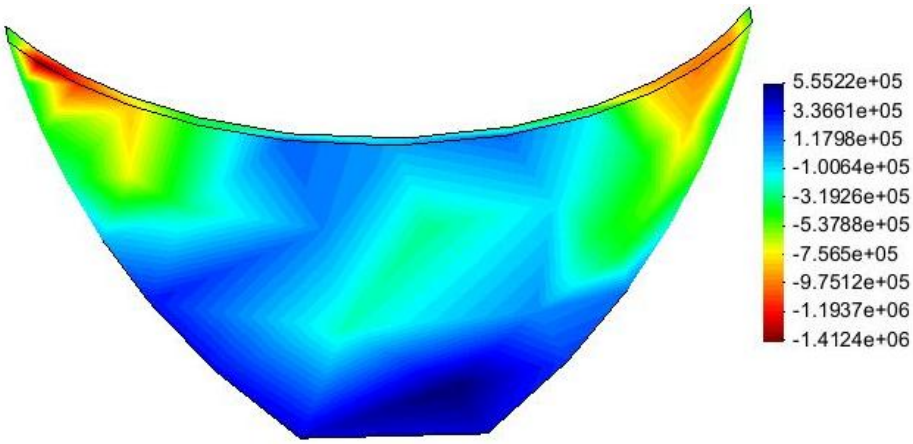

Fig. 6 Contours of principal stresses on upstream face of dam at time 9.2s (Unit: Pa)

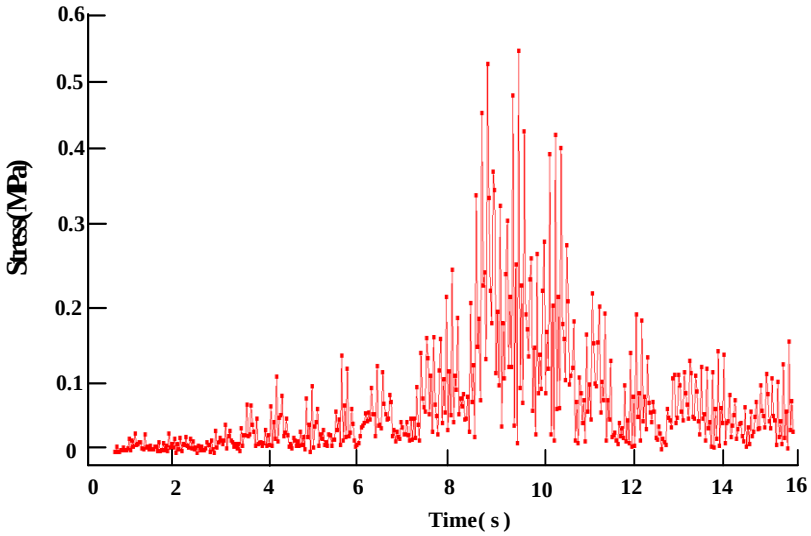

Fig. 7 Time-stress curve of point B in stream direction

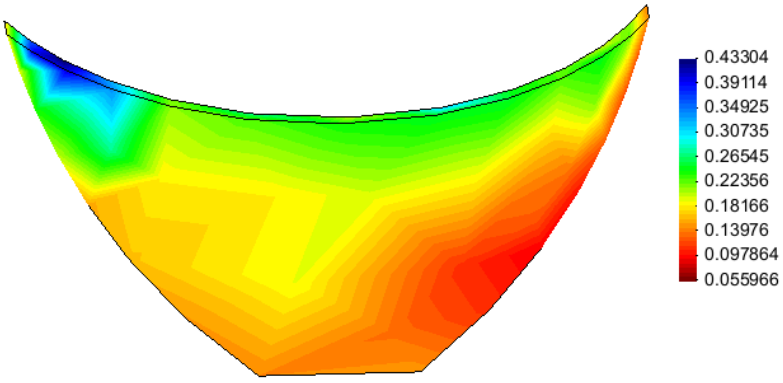

Fig. 8 Contours of Ω_y at the end of computational time

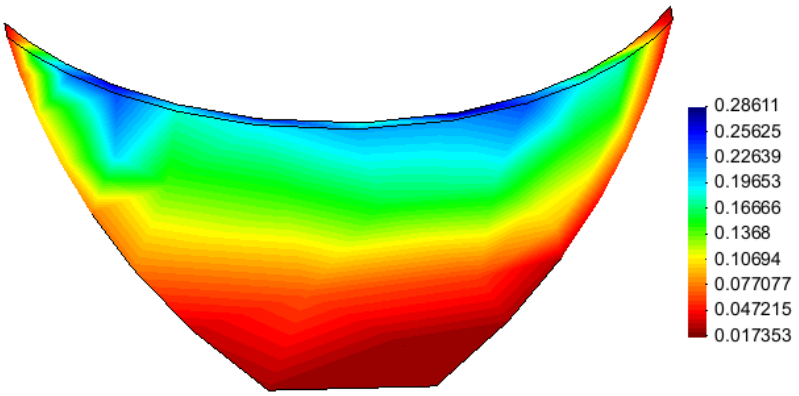

Fig. 9 Contours of Ω_x at the end of computational time

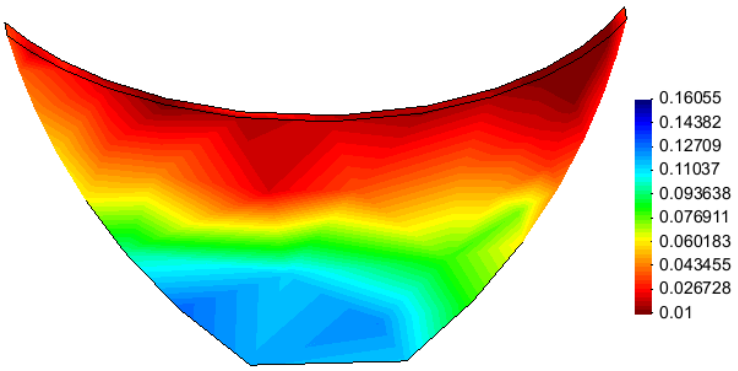

Fig. 10 Contours of Ω_z at the end of computational time

stream direction may reach the quantity of u=3.3cm, which agrees well with the results presented in Ref. (Dang 2008) (3.6cm). Fig. 5 shows the time-displacement curve of point A in stream direction. These results show that the damage model presented in this article is reasonable and feasible.

Fig. 6 shows the contours of principal stresses on upstream face of dam at time 9.2s. It can be seen that the phenomenon of stress concentration is quite distinctness. The maximum tensile stress of 1.41MPa is obtained in the upstream face near the left dam shoulder, which is smaller than the static tensile strength of the concrete and it agrees well with the results presented in Ref.(Dang 2008) (1.1MPa). Fig. 7 shows the time-stress curve of point B in stream direction. This indicates that the tensile stresses are the main reason to cause the damage of an arch dam under earthquake loading.

Fig. 8 shows the contours of Ω_y at the end of computational time. It can be seen that the maximum damage value along stream direction may reach the quantity of Ω_y=0.43304, which occurs at the top near the left dam shoulder.

Fig. 9 shows the contours of Ω_x at the end of computational time. It can be seen that the maximum damage value in the cross stream direction may reach the quantity of Ω_x = 0.28611, which occurs at the crest of the dam body.

Fig. 10 shows the contours of Ω_z at the end of computational time. It can be seen that the maximum damage value in vertical direction may reach the quantity of Ω_z =0.16055, which occurs at the dam-foundation rock interface.

From the above we can see that the higher values of the damage may occur at the crest of dam. Accordingly, the horizontal cracks might develop in the upper zone of an arch dam under strong earthquake, which has been verified by experimental studies (Zhou *et al*. 2000; Wang and Li 2007).

7. Conclusions

The simulation of damage process of high arch dam subjected to strong earthquake shocks is significant to the evaluation of its performance and seismic safety. This paper presents an

anisotropic damage model to simulate the safe behavior of an arch dam. Some process fields and other necessary information for the safety evaluation are obtained. The numerical results show that the seismic behaviour of concrete dams can be satisfactorily predicted. From these studies, following conclusions and understandings may be drawn:

(1) The anisotropic damage model developed in this paper is effective and feasible in simulating the safe behavior of an arch dam subjected to earthquake engineering.

(2) Numerical results show that the Buxi arch dam has a good performance of resisting seismic under designed earthquake and normal working conditions. Also it reveals that the damage of Buxi arch dam mainly owes to tension of concrete.

(3) In the present study, the anisotropic damage model should be subject to multifaceted experiments before their innovative significance can be fully verified. However, this research work has not been done due to the limitations of time, conditions, funds, etc. As such, there is still room for further refinement of the damage constitutive model of concrete in future studies.

References

Akköse, M., Bayraktar, A. and Dumanoğlu, A.A. (2007), "Reservoir water level effects on nonlinear dynamic response of arch dams", *J. Fluid Struct.*, **24**, 418-435.

Alves, S.W. and Hall, J.F. (2006), "System identification of a concrete arch dam and calibration of its finite element model", *Earthq. Eng. Struct.*, **35**, 1321-1337.

Bull, J.W. (1994), "Soil-structure interaction: numerical analysis and modelling", E &FN Spon, an imprint of Chapman & Hall, 2-6 Boundary Row, London SE1 8HN, UK.

Bazant, Z.P. (1987), "Snapback instability at crack ligament tearing and its implication for fracture micromechanics", *Cement Concrete Res.*, **17**(6), 951-967.

Chow, C.L. and Wang, J. (1988), "A finite element analysis of continuum damage mechanics for ductile fracture", *Int. J. Fracture*, **38**, 83-102.

Du, R.Q., Lin, G. and Zhang, Q. (2009), "Damage and fracture analysis of Dagangshan arch dam under strong earthquake", *Chinese J. Comput. Mech.*, **26**(3), 347-352. (in Chinese)

Dang, G.Q. (2008), "Analysis investigation on the seismic response of the system arch dam-reservoir water-foundation", *Xi'an University of Technology*, Xi'an. (in Chinese)

Dahlblom, O. and Ottosen, N.S. (1990), "Smeared crack analysis using a generalized fictitious crack model", *J. Eng. Mech. - ASCE*, **116**(1), 55-76.

Lotfi, V. and Espandar, R. (2004), "Seismic analysis of concrete arch dams by combined discrete crack and non-orthogonal smeared crack technique", *Eng. Struct.*, **26**, 27-37.

Lubliner, J., Oliver, J., Oller, S. and Onate, E. (1989), "A plastic-damage model for concrete", *Int. J. Solids Struct.*, **25**(3), 299-326.

Milan, J. (2011), "Damage and smeared crack models", Numerical modeling of concrete cracking, *CISM Courses Lectures*, **532**, 1-49.

Mirzabozorg, H. and Ghaemian, M. (2005), "Non-linear behavior of mass concrete in three-dimensional problems using a smeared crack approach", *Earthq. Eng. Struct. Dyn.*, **34**, 247-269.

Nor, H. and Abdul, H. (2010), "A concept development and proposed design procedure for rocking precast hollow core wall in warehouse", *J. Inst. Eng.*, **71**(2), 18-26.

Nayak, G. and Zienkiewicz, O.C. (1972), "Convenient form of stress invariants for plasticity", *J. Struct. Eng. ASCE*, 949-953.

Oliveira, S. and Faria, R. (2006), "Numerical simulation of collapse scenarios in reduced scale tests of arch dams", *Eng. Struct.*, **28**, 1430-1439.

Park, H. and Kim, J.Y. (2005), "Plasticity model using multiple failure criteria for concrete in compression", *Int. J. Solids Struct.*, **42**, 2303-2322.

Sevim, B., Bayraktar, A. and Altunışık, A.C. (2011), "Finite element model calibration of Berke arch dam using operational modal testing", *J. Vib. Control.*, **17**(7), 1065-1079.
Shahkarami, A., Delforouzi, M. and Salarirad, H. (2004), "Study of the compression and tension factors of safety with a 3-D FE Model for an arch dam and rock foundation: a case study of the Karun III arch dam in Iran", *Int. J. Rock. Mech. Min.*, **41**(3), 623-628.
Valliappan, S., Yazdchi, M. and Khalili, N. (1999), "Seismic analysis of arch dams-a continuum damage mechanics approach", *Int. J. Numer. Meth. Eng.*, **45**, 1695-1724.
Wang, J.T., Jin, F. and Zhang, C.H. (2011), "Seismic safety of arch dams with aging effects", *Sci. China. Technol. Sci.*, **54**(3), 522-530.
Westergaard, H.M. (1933), "Water pressure on dams during earthquakes", *Trans Am Soc Civ Eng* ,**98**(2),418-433.
Wang, H.L. and Li, D.Y. (2007), "Experimental study of dynamic damage of an arch dam", *Earthq. Eng. Struct. D*, **36**(3), 347-366.
Xue, X.H. (2008), "Non-linear damage mechanics theory of coupled fluid-solid with numerical analysis of geo-materials", *Zhejiang University*, Hangzhou. (in Chinese)
Zhou, J., Lin, G., Zhu, T., Jefferson, A.D. and Williams, F.W. (2000), "Experimental investigation into seismic failure of high arch dams", *J. Struct. Eng.*, **126**(8), 926-935.

CC